Hindawi
Advances in Civil Engineering
Volume 2021, Article ID 6656819, 10 pages
https://doi.org/10.1155/2021/6656819

Research Article

A Test Method for Creep Characteristics of Loess Based on the One-Dimensional Consolidator

Rongbin Huang,[1,2,3] **Shuangming Wang**,[1,3] **Shuancheng Gu**,[2] **and Zhengjun Mao**[4]

[1]*Post-Doctoral Mobile Station of Geological Resources and Geological Engineering, Xi'an University of Science and Technology, Xi'an, Shaanxi 710054, China*
[2]*School of Architecture and Civil Engineering, Xi'an University of Science and Technology, Xi'an, Shaanxi 710054, China*
[3]*Research Institute of Green Geology for Green Coal Mining, Xi'an, Shaanxi 710054, China*
[4]*College of Geology and Environment, Xi'an University of Science and Technology, Xi'an 710054, China*

Correspondence should be addressed to Rongbin Huang; huangrongbin@xust.edu.cn

Received 17 December 2020; Accepted 27 September 2021; Published 11 October 2021

Academic Editor: Bingxiang Yuan

When the traditional one-dimensional consolidator is used to study the creep characteristics of loess, due to the hoop effect of the ring cutter, only the attenuation creep stage and stable creep stage of loess can be studied, but the accelerated creep stage cannot be presented. In order to avoid the influence of drilling on the creep characteristics of loess, the paper improves the consolidation instrument by drilling holes along the diameter direction in the center of the sample to provide artificial space for soil failure. At the same time, the sample size is increased to ensure that the diameter of the sample is greater than five times of the diameter of the borehole, so as to avoid the influence of drilling on the creep characteristics of loess. The creep characteristics of loess are studied by step loading (vertical pressure at all levels is 125 kPa, 175 Pa, 225 kPa, and 275 kPa), and the whole creep process characteristic curves of loess under different stress conditions are obtained. An endoscope was placed in the hole to observe the deformation and failure characteristics of loess in different stages of creep. This method makes up for the defect that the traditional one-dimensional consolidator cannot obtain the whole process characteristics of loess creep. At the same time, it has the advantages of simple operation, less external influence factors, stronger data reliability, and can directly observe the changes of loess creep soil. It has a beneficial role in promoting the experimental research of loess creep characteristics.

1. Introduction

The loess covers a vast area, with a total area of 13 million km^2, covering more than 9.3% of the global continental area. The total area of loess in China is about 640000 km^2, accounting for 6.3% of the total land area, of which loess is the most widely distributed in Western China, accounting for 50%–60% of the total area in the western region. The creep behavior of loess is one of the most important problems to be studied [1–7].

For a long time, many scholars have made a lot of progress in the experimental study of soil long-term deformation. Bjerrum carried out creep test on Norwegian marine clay and analyzed the micromechanism of cohesive soil during long-term deformation [8]. Through a series of one-dimensional consolidation and isotropic consolidation tests, Mesri and Godlewski pointed out that the soil with high compressibility in the main consolidation stage has relatively high compressibility in the secondary consolidation stage [9]. Chang et al. pointed out that when the effective stress increases to the preconsolidation pressure, both the secondary consolidation coefficient and the compression index increase. When the effective stress exceeds the preconsolidation pressure, the coefficient of secondary consolidation and compressibility do not change [10]. Wang et al. carried out a series of creep tests and obtained the influence of moisture content, dry density, and deviatoric stress on the creep characteristics of undisturbed, remolded,

and saturated loess [11]. Zhu and Li carried out in situ monitoring and laboratory test by using the soil resistivity consolidation tester to reveal the creep mechanism of the loess high-fill foundation from the microperspective [12]. He studied the correlation characteristics of different confining pressures, water contents, and dry densities on the change of loess deformation with time through the triaxial compression test of remolded loess [13]. Xiao et al. took unsaturated silty clay as an example, carried out triaxial compression consolidation drainage creep test under matrix suction control, constructed the elastomer and fractional viscous body considering matrix suction, and established the creep constitutive model of unsaturated silty clay considering matrix suction [14]. Ge et al. put forward a creep model conforming to the deformation law of compacted loess based on the long-term creep test of loess with a one-dimensional consolidation instrument [15, 16]. Zhang et al. studied the creep effect of loess through the one-dimensional consolidation creep test and analyzed the effects of water content and compactness on loess creep [17]. Yang et al. and Zhang studied the compactness and moisture content characteristics of remolded loess by using the one-dimensional confined compression experiment and analyzed the creep law of soil samples [18, 19]. Chen studied the creep properties of remolded loess by using the one-dimensional consolidation instrument and three-dimensional consolidation instrument. The above tests showed two-stage creep characteristics [20].

Many scholars have carried out in-depth research on the creep characteristics of loess and achieved a series of excellent results [21–27]. In practical engineering, loess is basically multidimensional stress. However, through the study of loess creep under one-dimensional stress, we can better understand the creep characteristics of loess under multi-dimensional stress, so the relevant research is still of great significance. In addition, it is easier to control the load and eliminate the external factors, so it is easier to draw valuable conclusions. Based on the long-term creep test of loess with the one-dimensional high-pressure consolidator, some scholars have proposed an empirical model that conforms to the deformation law of compacted loess [28–31]. According to the results of the unidirectional consolidation test of loess, some researchers compared undisturbed loess with disturbed loess and obtained creep curves and characteristic parameters of loess creep characteristics [32–34]. Some researchers have carried out unidirectional consolidation tests on loess which has experienced freeze-thaw cycles and studied the effects of freeze-thaw cycles and normal pressure on the consolidation creep characteristics of freeze-thaw loess [35–37].

However, during the loess creep test with the one-dimensional consolidation tester, in addition to providing lateral confining pressure for the specimen, the lateral deformation of the specimen will also be limited under the hoop action of the ring cutter. Under the above joint action, only vertical compression settlement can occur in the test process, and the subsidence rate gradually decreases to zero, which means that the above tests can only show the characteristics of deceleration creep, but not the accelerated creep stage. Therefore, the paper drilled holes along the diameter direction in the center of the sample to provide artificial soil failure space. The specimen size was increased to ensure that the drilling does not affect the overall stress distribution of the specimen. At the same time, an endoscope was placed in the borehole to observe the deformation and failure characteristics of loess in various stages of creep.

2. Test Principle

The method of drilling holes in the middle of the sample is used to provide deformation space for loess creep. According to Saint Venant's principle and the elastic stress solution of underground cavern, the excavation of circular cavern has a significant impact on the surrounding rock within 5 times the tunnel diameter, and the surrounding rock stress outside 5 times the tunnel diameter can be approximately the original rock stress. Therefore, the sample drilling diameter shall meet the following requirements:

$$r_0 < \frac{1}{5} r_1, \tag{1}$$

where r_0 is the drilling radius and r_1 is the ring cutter radius.

The hole can maintain self-stability under the external load. In the creep test of loess under specific confining pressure, it is necessary to ensure that the borehole remains stable at the moment of loading.

On the premise of meeting the above conditions, the larger value of borehole diameter should be adopted to make the test results more obvious. According to the above principle, the experimental design is carried out, and the test schematic diagram is shown in Figure 1. The size of the ring cutter increased from 2.0 cm × 6.18 cm (height × diameter) to 6.0 cm × 6.18 cm. Holes were drilled along the diameter in the center of the sample to provide the deformation space for loess creep, as shown in Figure 2. During the test, in order to obtain the deformation and failure mode of soil in real time, an endoscope was used to collect photos, as shown in Figure 3.

3. Test Procedure

(1) In order to separate the sample from the ring cutter after the test, attention should be paid to the lubrication treatment of the wall of the ring cutter.

(2) The drill bit with the specified diameter is selected to drill the sample along the diameter. Drilling should be carried out slowly and uniformly to reduce disturbance to the sample. After the completion of drilling, the hole should be cleaned to ensure that the surface around the hole is smooth, and there are no soil particles in the hole.

(3) The retaining ring, permeable plate, and thin filter paper are placed in the consolidation container. Install the ring cutter with the sample into the

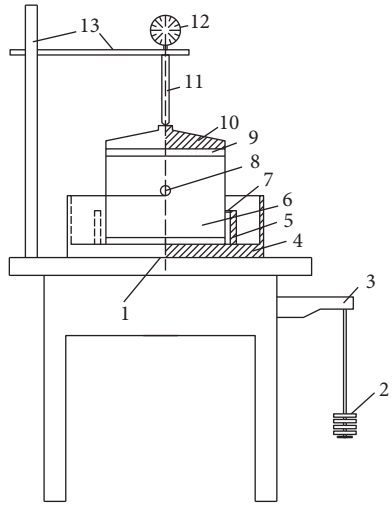

1-test platform
2-loading weight
3-transfer lever
4-water tank
5-retaining ring
6-sample
7-ring cutter
8-sample drilling
9-permeable stone
10-pressure upper cover
11-loading guide rod
12-displacement meter
13-displacement meter frame

Figure 1: Schematic diagram of the test: 1, test platform; 2, loading weight; 3, transfer lever; 4, water tank; 5, retaining ring; 6, sample; 7, ring cutter; 8, sample drilling; 9, permeable stone; 10, pressure upper cover; 11, loading guide rod; 12, displacement meter; 13, displacement meter frame.

retaining ring and put on the guide ring. Thin filter paper, permeable plate, and pressurized upper cover are placed on the sample in turn. Place the consolidation vessel in the center of the pressurized frame so that the pressurized upper cover is aligned with the center of the pressurized frame. Finally, install the dial indicator.

(4) Apply 1 kPa prepressure to make the sample contact with the upper and lower parts of the instrument. Adjust the dial indicator or sensor to zero or measure the initial reading.

(5) Group loading is implemented. The vertical load values are 125 kPa, 175 kPa, and 225 kPa, respectively, and one group of parallel tests is set to verify the accuracy of the test results.

(6) According to the following time sequence, the height change time of the sample is 6 s, 15 s, 1 min, 2 min, 4 min, 6 min 15 s, 9 min, 12 min 15 s, 16 min, 20 min 25 s, 25 min, 30 min 15 s, 36 min, 42 min 15 s, 49 min, 64 min, 100 min, 2 h, 3 h, 4 h, etc., until stable. The stability criterion of the paper is that the soil deformation within 24 hours is less than 0.01 mm.

(7) After the test, the sample is separated from the ring cutter. The samples were sliced at the quarter diameter, half diameter, and diameter. The distribution law of plastic failure of soil around each section of the borehole was recorded.

4. Analysis of Test Examples

Taking the loess in Xi'an area of China as an example, the creep characteristics of loess are studied. In the experiment, the inner diameter of the ring knife is 61.8 mm, and the height is 60 mm. According to the drilling diameter requirements, the drilling diameter is determined to be 8 mm, and the drilling position is at the center line of the ring cutter height. The main physical and mechanical parameters of the sample are shown in Table 1.

In order to explore the deformation and failure law of specimens under different vertical loads, the vertical loads of 100 kPa, 200 kPa, 300 kPa, 400 kPa, 500 kPa, 600 kPa, 700 kPa, and 800 kPa were applied to the samples. After the deformation is basically stable, the deformation and failure modes of the borehole under the current stress state are photographed by using a peep. After the above load is applied, the soil sample is taken out from the ring cutter. Soil samples were sliced in different directions to analyze the plastic failure law of soil.

Table 2 shows the failure modes of the samples under different vertical loads. Through the analysis, it is preliminarily determined that the maximum vertical load to keep the borehole stable is between 200 kPa and 300 kPa. It can be seen from Figure 4 that, after loading 800 kPa, the specimen is obviously compressed, and the drilling hole moves downward as a whole.

Figure 5 shows the failure pattern of loess along the drilling direction. The main failure mode is the surface soil spalling, and the failure range is basically symmetrical along the borehole.

Figure 6 shows the failure pattern of the sample at different positions perpendicular to the drilling direction. The range of the plastic zone at 1/4 radius is relatively small, the borehole becomes smaller, and there is spalling soil in the borehole. The plastic zone at 1/2 radius is obviously expanded, and the drilling hole changes from circular to oval. The drill holes in the section at the diameter are oval. The plastic zone is further expanded and distributed symmetrically in saddle shape.

Figure 7 shows the distribution of the plastic zone near the diameter. The plastic zone is symmetrically distributed in the upper part of the borehole in the form of bimodal. The maximum radius of the plastic zone is about 45° with the horizontal direction. The maximum radius of the plastic zone is about 2.9 times of the drilling radius. The radius of the plastic zone directly above the borehole is about 1.7 times of the borehole radius. The radius of the plastic zone on both sides of the horizontal direction of the borehole is about 2.0 of the borehole radius. Through the parallel contrast test, it is found that the above laws are universal. The analysis shows that the hole near the ring cutter is obviously affected by the boundary of the ring cutter, which leads to the difference between the deformation and failure of the drilling hole at the central position. The maximum radius of the plastic zone is about 45° with the positive angle of the Y-axis. The failure mode is consistent with the boundary line of the plastic zone of the soil sample calculated by relevant theories.

Figure 2: Schematic diagram of the ring knife and soil sample.

Figure 3: 5.5 mm snake tube endoscope.

Table 1: Main physical and mechanical parameters of loess samples.

Natural density (g/cm^3)	Lateral pressure coefficient	Liquid limit (%)	Plastic limit (%)	Moisture content (%)	Internal friction angle (°)	Cohesion (kPa)
1.67	0.408	27.22	17.25	23.8	24.4	45.6

Figure 8 shows the creep characteristics of loess under different loading conditions. When the vertical load is 125 kPa and 175 kPa, the samples show typical attenuation creep characteristics: the soil strain rate gradually decreases from the maximum value to 0, and the soil strain tends to a fixed value. When the load is 225 kPa, the specimen first experiences the decay creep and the stable creep. When the specimen is deformed to point *a*, the strain rate increases and enters the accelerated creep stage. When the load is 275 kPa, the creep law of the specimen is basically consistent with that at 225 kPa. However, due to the increase of vertical load, the total strain increases, and the time from the stable creep stage to the accelerated creep stage is advanced, and the strain increase rate in the accelerated creep stage increases.

When establishing the creep constitutive model of loess based on the test results, it is necessary to consider not only accurately reflecting the actual creep characteristics of soil but also minimizing the undetermined parameters in the model.

Table 2: Failure modes of drilling holes under different vertical loads.

Load (kPa)	Pictures and introduction	Load (kPa)	Pictures and introduction
0	 Ring cutter size: height 60 mm and diameter 61.8 mm. Drilling size: 8 mm in diameter. Drill along the ring cutter diameter at 30 mm height to ensure smooth drilling.	100	 After loading, the borehole did not change significantly.
200	 The surface of the borehole began to be uneven.	300	 The surface of the borehole is obviously uneven. In the upper right part of the borehole, skin exfoliation first appeared. According to the image feedback, when the iron bar coated with vaseline is gently in contact with the surface of the borehole, soil particles can be found attached, which indicates that soil is damaged and dropped into the hole.
400	 The surface of the borehole is further roughened.	500	 There was a large area of exfoliation on the drilling surface. The hole is flattened; that is, the hole circumference changes from circular to oval.
600	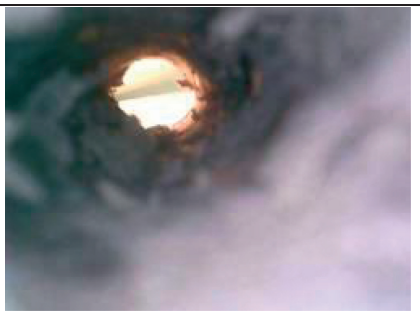 There was a large area of exfoliation on the drilling surface.	700	 There was a large area of exfoliation on the drilling surface.

Table 2: Continued.

Load (kPa)	Pictures and introduction	Load (kPa)	Pictures and introduction
800			The surface of the borehole peeled off in large area and gradually filled the whole borehole.

(a) (b)

Figure 4: Deformation pattern of the sample after unloading. (a) The form of hole sinking. (b) The overall sinking pattern of the sample.

Figure 5: Failure pattern of loess along the drilling direction.

Burgers model can be used to describe the soil with instantaneous elastic deformation, attenuation creep, constant velocity creep, and residual deformation after unloading. At the same time, the model parameters are less, which is convenient for theoretical analysis. Therefore, Burgers model is used to analyze the creep characteristics of loess. Since Burgers model is

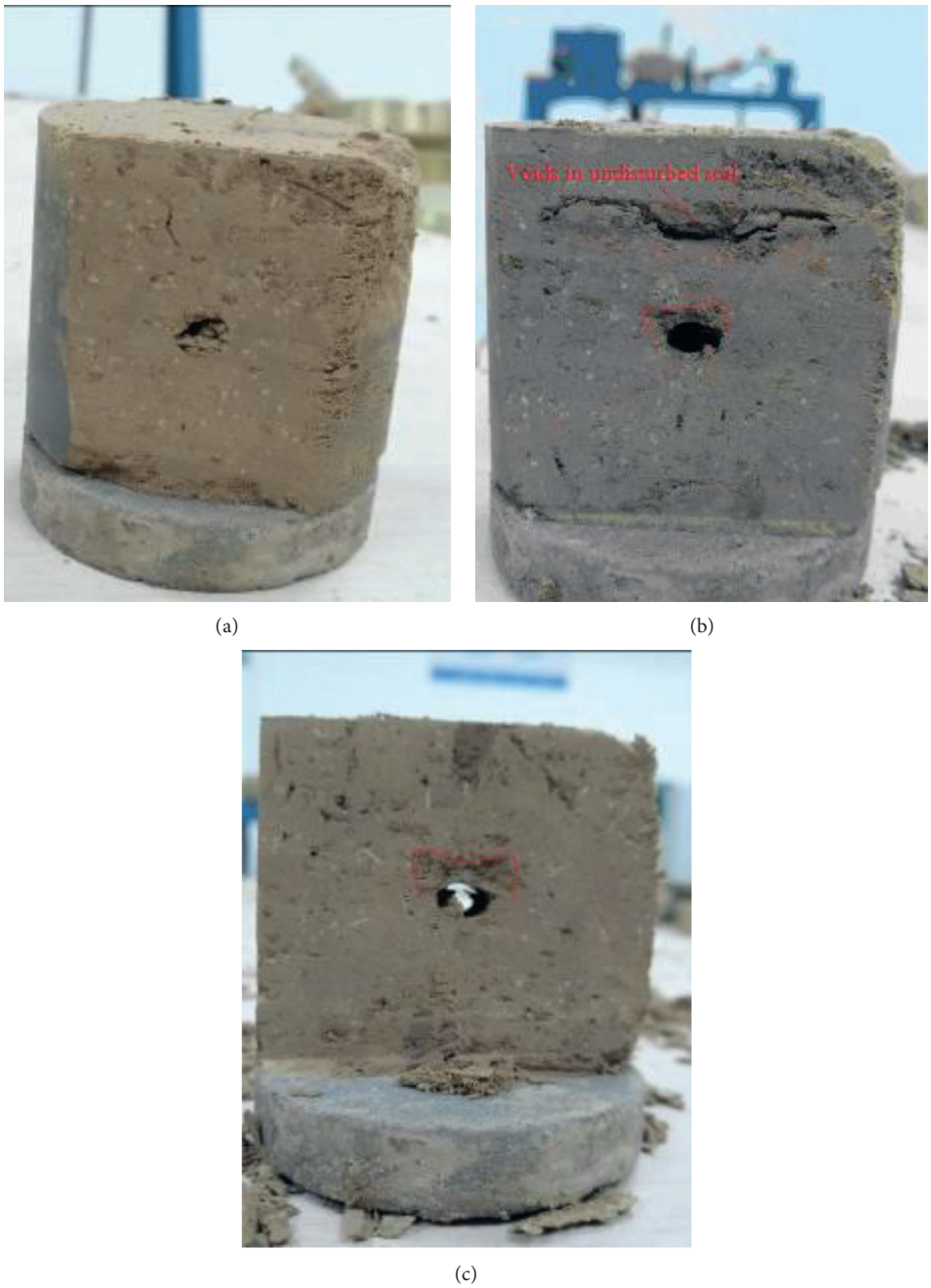

(a) (b) (c)

Figure 6: Failure mode of the slice perpendicular to the drilling direction: (a) failure mode of the drilling hole at the 1/4 radius section, (b) failure mode of the drilling hole at the 1/2 radius section, and (c) failure mode of the drilling hole at the diameter section.

a viscoelastic model, the relevant data of the accelerated creep stage are excluded for analysis when calculating the model parameters (Figure 9).

The constitutive equation of the Burgers model is as follows:

$$\varepsilon = \frac{\sigma}{E_1} + \frac{\sigma}{\eta_1} t + \frac{\sigma}{E_2}\left(1 - e^{-(E_2/\eta_2)t}\right). \quad (2)$$

Figure 10 and Table 3 show the fitting results and model parameters of the Burgers model. Burgers model can accurately characterize the creep characteristics of loess. It can be seen that the application of the test method proposed in this paper, combined with the Burgers model, can scientifically analyze the deformation law of loess in elastic deformation, attenuation creep, constant velocity creep, and other stages.

5. Discussion

Compared with the traditional one-dimensional consolidation apparatus, the creep test method proposed in this paper can obtain the whole creep process characteristics of loess. At the same time, the method has the advantages of

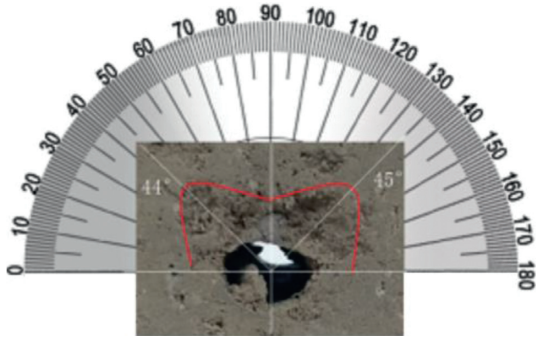

Figure 7: Plastic failure of soil around the drilling hole.

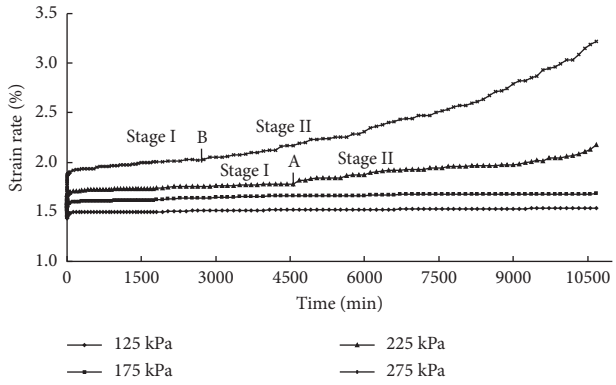

Figure 8: Creep curves of loess samples. Stage I: decay creep stage and stable creep stage. Stage II: accelerated creep stage.

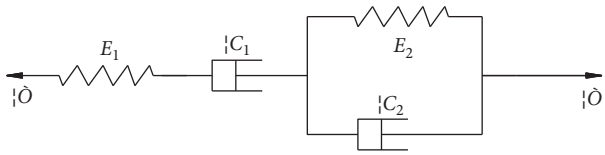

Figure 9: Burgers model.

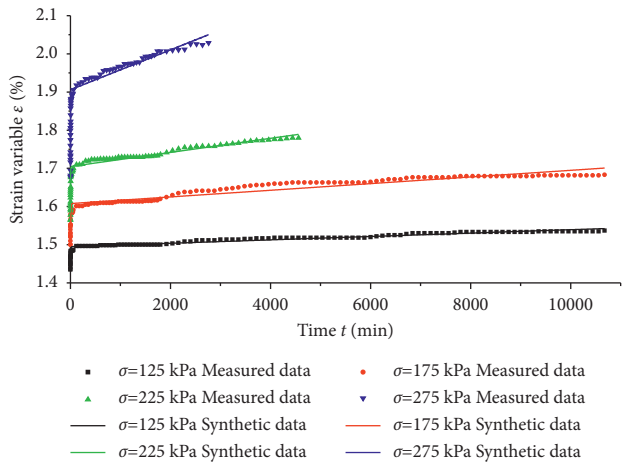

Figure 10: Fitting analysis with the Burgers model.

Table 3: Parameters of the Burgers model.

Load (kPa)	E_1 (kPa)	η_1 (kPa.h)	E_2 (kPa)	η_2 (kPa.h)	Variance
275	38.77	68728.52	372.02	31.35	0.93326
225	30.76	48661.80	140.63	114.95	0.97118
175	31.04	50761.42	188.37	69.53	0.98195
125	28.93	57486.59	251.55	48.68	0.97323

simple operation, less external factors, and real-time observation of the internal failure mode of soil. It provides a new method for the further study of loess creep characteristics and has a beneficial role in promoting the related research.

The test method described in this paper is generally applicable to the study of creep characteristics of general loess. The experimental results provide a basis for the study of the long-term strength change of loess, the long-term deformation law of loess, and the long-term mechanical characteristics of the supporting structure under loess geological conditions.

However, this experiment only considers the vertical load conditions, so it cannot study the creep characteristics of loess under complex stress conditions. At the same time, because the collapsibility of loess has a direct impact on the deformation and failure of the borehole, it is impossible to accurately distinguish collapsible deformation from creep deformation. Therefore, the creep characteristics of collapsible loess cannot be studied by this method.

In the next step, it is necessary to systematically study the creep characteristics of loess under the influence of key parameters such as moisture content and porosity.

6. Conclusion

(1) Based on the one-dimensional consolidator, a creep test method of loess is proposed in this paper. Three complete stages of the loess creep process can be obtained by this method. At the same time, the change of soil mass can be observed in the whole process of creep, so as to understand the creep characteristics of loess.

(2) At the moment of loading, the sample deforms instantaneously. With the increase of time, the deformation also increases, and the higher the stress level, the greater the instantaneous deformation and creep deformation.

(3) With the increase of vertical load, soil debris appears first on the surface of the borehole, and then there are complex cracks around the hole. At about 45° above the hole inclination, the soil mass first exfoliated, and then the spalling area diffused in a large range until the whole hole was destroyed. In this process, the shape of the borehole becomes flat and finally changes from round to oval.

Data Availability

The data used to support the findings of this study are available from the corresponding author upon request.

Conflicts of Interest

The authors declare that they have no conflicts of interest.

Acknowledgments

This work was financially supported by the China Postdoctoral Science Foundation (no. 2019M663936XB), the Scientific Research Plan for Local Special Service of Shaanxi Provincial Education Department (no. 19JC027), the Shaanxi Provincial Key Research and Development Plan (no. 2020SF-379), the Scientific Research Program funded by Shaanxi Provincial Education Department (no. 19JK0399), and Key R&D Plan of Ningxia Hui Autonomous Region (no. 2020BEG03023).

References

[1] X. Xie, S. Qi, F. Zhao, and D. Wang, "Creep behavior and the microstructural evolution of loess-like soil from Xi'an area, China," *Engineering Geology*, vol. 236, pp. 43–59, 2018.

[2] H. Tang, Z. Duan, D. Wang, and Q. Dang, "Experimental investigation of creep behavior of loess under different moisture contents," *Bulletin of Engineering Geology and the Environment*, vol. 79, no. 1, pp. 411–422, 2020.

[3] X. G. Wang, J. D. Wang, H. B. Zhan, P. Li, H. Qiu, and S. Hu, "Moisture content effect on the creep behavior of loess for the catastrophic Baqiao landslide," *Catena*, vol. 187, 2020.

[4] X. Yuan, L. Xiong, L. Zhai et al., "Transparent synthetic soil and its application in modeling of soil-structure interaction using optical system," *Frontiers of Earth Science*, vol. 7, no. 276, 2019.

[5] H. Tang, D. P. Wang, and Z. Duan, "New maxwell creep model based on fractional and elastic-plastic elements," *Advances in Civil Engineering*, vol. 2020, Article ID 9170706, 11 pages, 2020.

[6] J. D. Wang, X. G. Wang, H. B. Zhan, H. Qiu, and S. Hu, "A new superlinear viscoplastic shear model for accelerated rheological deformation," *Computers and Geotechnics*, vol. 114, 2019.

[7] C. H. Zhu and N. Li, "Ranking of influence factors and control technologies for the post-construction settlement of loess high-filling embankments," *Computers and Geotechnics*, vol. 118, 2020.

[8] L. Bjerrum, "Engineering geology of Norwegian normally-consolidated marine clays as related to settlements of buildings," *Géotechnique*, vol. 17, no. 2, pp. 83–118, 1967.

[9] G. Mesri and P. M. Godlewski, "Time- and stress-compressibility interrelationship," *Journal of the Geotechnical Engineering Division*, vol. 103, no. 5, pp. 417–430, 1977.

[10] Z. Chang, H. Gao, F. Huang, J. Chen, J. Huang, and Z. Guo, "Study on the creep behaviours and the improved Burgers model of a loess landslide considering matric suction," *Natural Hazards*, vol. 103, no. 1, pp. 1479–1497, 2020.

[11] S. H. Wang, Y. S. Luo, and X. H. Dong, "Experimental study of shear creep characteristics of loess," *Chinese Journal of Rock Mechanics and Engineering*, vol. 29, no. S1, pp. 3088–3092, 2010.

[12] C. H. Zhu and N. Li, "Mesoscopic deformation mechanism of loess high-fill foundation based on soil electrical resistivity," *Chinese Journal of Rock Mechanics and Engineering*, vol. 32, no. 3, pp. 640–648, 2013.

[13] H. He, *Study on Loess Deformation Characteristics and Engineering Application Considering Time Effect*, Xi'an University of Architecture and Technology, Xi'an, China, 2017.

[14] H. J. Xiao, P. Hu, and C. Y. Zeng, "Experimental study on creep mechanical properties of unsaturated soil and sectional simulation," *Science Technology and Engineering*, vol. 20, no. 22, pp. 9133–9139, 2020.

[15] M. M. Ge, N. Li, and J. G. Zheng, "Creep model of compacted loess based on one-dimensional consolidation test," *Geotechnical Mechanic*, vol. 250, no. 11, pp. 3164–3170, 2015.

[16] L. Li, "3D creep constitutive identification method for Q3 undisturbed loess in ground fissure zone," *Journal of Underground Space and Engineering*, vol. 13, no. 4, pp. 905–912, 2017.

[17] Y. H. Zhang, F. Gao, and G. S. Lu, "Numerical simulation of high fill foundation settlement based on loess creep test," *Science Technology and Engineering*, vol. 18, no. 30, pp. 220–227, 2018.

[18] P. Yang, M. H. Wu, and D. X. Xu, "Experimental study on influence of water content on deformation characteristics of remolded loess," *Journal of Engineering Geology*, vol. 2015, no. 6, pp. 1066–1071, 2015.

[19] S. W. Zhang, *One Dimensional Consolidation and Creep Characteristics of Unsaturated Remolded Loess*, Xi'an University of Technology, Xian, China, 2018.

[20] Y. Z. Chen, "Study on one dimensional and three dimensional creep characteristics of remolded loess," *Construction Technology*, vol. 2017, no. 46, pp. 1197–1201, 2017.

[21] J. Wang, Y. Xu, Y. Ma, S. Qiao, and K. Feng, "Study on the deformation and failure modes of filling slope in loess filling engineering: a case study at a loess mountain airport," *Landslides*, vol. 15, no. 12, pp. 2423–2435, 2018.

[22] H. T. Cheng, B. J. Liu, and Y. L. Xie, "Deformation characteristics of remolded loess," *Journal of Chang'an University (Natural Science Edition)*, vol. 28, no. 5, pp. 31–34, 2008.

[23] Y. K. Wu, H. W. Chen, and Z. Z. Zhang, "Characteristics of saturated loess and rheological model of unsaturated loess in Xi'an," *Rock and Soil Mechanics*, vol. 25, no. 7, pp. 1143–1146, 2004.

[24] A. Singh and J. K. Mitchell, "General stress-strain-time function for soils," *Soils and Foundations*, vol. 94, no. 1, pp. 21–46, 1992.

[25] X. Yuan, M. Sun, L. Xiong, Q. Luo, S. P. Pradhan, and H. Li, "Investigation of 3D deformation of transparent soil around a laterally loaded pile based on a hydraulic gradient model tes," *Journal of Building Engineering*, vol. 28, 2020.

[26] Q. J. Zhou and X. P. Chen, "Experimental study on creep characteristics of soft soil," *Chinese Journal of Geotechnical Engineering*, vol. 28, no. 5, pp. 626–629, 2006.

[27] R. G. Gu and Y. G. Fang, "Experiment study on effects of mineral composition on rheological characteristics of soft clayey soil," *Rock and Soil Mechanics*, vol. 28, no. 12, pp. 2682–2685, 2007.

[28] L. Tang and M. Z. Wu, "Experimental test on rheological properties of soft soil," *Subgrade Engineering*, vol. 2007, no. 5, pp. 106–108, 2007.

[29] Z. C. Wang, Y. S. Luo, W. B. Luo, and X. Deng, "Mechanical characterization and parameter identification of rheological deformation of subgrade compacted soil," *Chinese Journal of*

Rock Mechanics and Engineering, vol. 30, no. 1, pp. 209–216, 2011.

[30] C. Yang, R. Wang, and Q. S. Meng, "Study of soft soil triaxial shear creep test and model analysis," *Rock and Soil Mechanics*, vol. 33, no. 1, pp. 106–110, 2012.

[31] G. X. Mei, J. M. Zai, W. B. Zhao, and J. Yin, "Settlement prediction method considering creep," *Chinese Journal of Geotechnical Engineering*, vol. 26, no. 3, pp. 416–418, 2004.

[32] Z. Y. Yin, "Modeling of time-dependent behaviour of soft soil using simple elasto-viscoplastic model," *Chinese Journal of Geotechnical Engineering*, vol. 30, no. 6, pp. 881–887, 2008.

[33] E. X. Song and G. X. Cao, "Characteristics and simplified calculation method of creep settlement of high fill foundation in mountain area," *Rock and Soil Mechanics*, vol. 33, no. 6, pp. 1711–1718+1723, 2012.

[34] Y. Yao, L. Kong, and J. Hu, "An elastic-viscous-plastic model for overconsolidated clays," *Science China Technological Sciences*, vol. 2013, no. 56, pp. 441–457, 2013.

[35] X. Yuan, M. Sun, Y. X. Wang, I. Zhai, Q. Liu, and X. Zhang, "Full 3D displacement measuring system for 3D displacement field of soil around a laterally loaded pile in transparent soil," *International Journal of Geomechanics*, vol. 19, no. 5, Article ID 04019028, 2019.

[36] Y. Zhang, Y. Q. Xue, J. C. Wu, and X. Y. Shi, "Creep model of saturated sands in oedometer tests," *Soil and Rock Behavior and Modeling*, vol. 2006, no. 1, pp. 328–334, 2006.

[37] Z. Zhou, W. Ma, S. Zhang, H. Du, Y. Mu, and G. Li, "Multiaxial creep of frozen loess," *Mechanics of Materials*, vol. 95, pp. 172–191, 2016.